Shape evolution of the highly deformed ^{75}Kr nucleus examined with the Doppler-shift attenuation method

T. Trivedi,[1] R. Palit,[2] D. Negi,[3] Z. Naik,[2] Y.-C. Yang,[4] Y. Sun,[4,5] J. A. Sheikh,[5,6,7] A. Dhal,[8] M. K. Raju,[9] S. Appannababu,[10] S. Kumar,[11] D. Choudhury,[12] K. Maurya,[1] G. Mahanto,[3] R. Kumar,[3] R. P. Singh,[3] S. Muralithar,[3] A. K. Jain,[12] H. C. Jain,[2] S. C. Pancholi,[3] R. K. Bhowmik,[3] and I. Mehrotra[1]

[1]*Department of Physics, University of Allahabad, Allahabad 211001, India*
[2]*Department of Nuclear and Atomic Physics, Tata Institute of Fundamental Research, Mumbai 400005, India*
[3]*Inter University Accelerator Centre, New Delhi 110067, India*
[4]*Department of Physics, Shanghai Jiao Tong University, Shanghai 200240, People's Republic of China*
[5]*Department of Physics and Astronomy, University of Tennessee, Knoxville, Tennessee 37996, USA*
[6]*Physics Division, Oak Ridge National Laboratory, Post Office Box 2008, Oak Ridge, Tennessee 37831, USA*
[7]*Department of Physics, University of Kashmir, Srinagar 190006, India*
[8]*Department of Physics, Banaras Hindu University, Varanasi 221005, India*
[9]*Department of Nuclear Physics, Andhra University, Visakhapatnam 530003, India*
[10]*Department of Physics, MS University of Baroda, Vadodara 390002, India*
[11]*Department of Physics and Astrophysics, University of Delhi, Delhi 110007, India*
[12]*Department of Physics, IIT Roorkee, Roorkee 247667, India*

(Received 31 July 2009; revised manuscript received 28 September 2009; published 28 October 2009; corrected 2 November 2009)

High-spin states of the ^{75}Kr nucleus have been populated via the ^{50}Cr(^{28}Si,$2pn$)^{75}Kr reaction at an incident beam energy of 90 MeV. Lifetimes of nine states up to spin $I = 33/2$ for the positive-parity band and seven states up to $I = 27/2$ for the negative-parity band have been measured using the Doppler-shift attenuation method. The deduced transition quadrupole moments Q_t of these bands have been compared to the projected shell-model calculations to gain insight into the evolution of collectivity for the two experimentally studied bands in ^{75}Kr.

DOI: 10.1103/PhysRevC.80.047302 PACS number(s): 21.10.Tg, 21.10.Re, 21.60.Cs, 27.50.+e

Atomic nuclei exhibit a rich variety of phenomena due primarily to changes in the shell structure with changes in particle number and excitation energy. The neutron-deficient isotopes with $A \sim 70$–80 in particular have attracted considerable attention because of the observation of large deformation and shape coexistence at low excitation energies [1–3]. In this mass region, dramatic competition among different shapes occurs because of the oblate deformed shell gaps at N or $Z = 34$ and 36, the prolate deformed shell gaps at N or $Z = 34$ and 38, and the spherical shell gap at N or $Z = 40$ [4]. Previous studies of lifetimes in ^{77,78}Kr [5,6] and ^{80,81}Y [7,8] show loss of collectivity near the band-crossing region, indicating that the shape changes in each band from prolate at low spin to triaxial above the first rotational alignment. These results are in good agreement with theoretical predictions of models such as the Hartree-Fock-Bogoliubov cranking model and the projected shell model [7].

In recent years, various structural similarities have also been observed in lighter neutron-deficient even Z and odd N nuclei, especially in ^{73}Se [9], ^{77}Kr [5], and ^{77}Sr [10], because of the occupation of valence neutrons in the unique-parity $g_{9/2}$ orbital. The ^{75}Kr nucleus lies between the two well-studied ^{76}Kr and ^{74}Kr nuclei, with greatest deformation among all the krypton isotopes. Previous recoil distance lifetime measurements [11,12] for the low-spin states of both positive- and negative-parity bands revealed that ^{75}Kr has a large quadrupole deformation of $\beta_2 \approx 0.40$. The purpose of the present work is to understand the evolution of nuclear shape with increasing angular momentum in ^{75}Kr through the measurement of lifetimes of high-spin states. These bands exhibit a slight reduction in collectivity after the band crossing. The properties of these bands observed up to high spins are compared with those obtained using projected shell-model (PSM) [13,14] calculations.

The excited states of the ^{75}Kr nucleus have been populated via the ^{50}Cr(^{28}Si,$2pn$) fusion evaporation reaction at an incident beam energy of 90 MeV using the 15-UD Pelletron accelerator [15] at the Inter University Accelerator Centre, New Delhi, India. The target consisted of $\sim$550 μg/cm^2 isotopically enriched 96% ^{50}Cr with $\sim$12 mg/cm^2 gold backing. The de-exciting γ rays were detected with the Indian National Gamma Array [16] consisting of 17 Compton-suppressed clover detectors at the time of the experiment. The clover detectors were arranged in five rings, at 32°, 57°, 90°, 123°, and 148° with respect to the beam direction. For the application of the Doppler-shift attenuation method, line shapes were obtained from the background-subtracted spectra projected from matrices consisting of events in the 148° or 32° detectors along one axis and all other detectors along the second axis. These matrices contained approximately 3×10^8 and 1.5×10^8 coincidence events, respectively.

The transitions reported in the level scheme developed by Skoda *et al.* [12] were identified and used as reference data for this measurement. For analyzing the line shapes of different transitions of ^{75}Kr, mentioned in Table I, we have used the program LINESHAPE developed by Wells [17]. The Monte Carlo simulation technique has been used in this program for the velocity and directional history of a series of recoiling nuclei

TABLE I. Experimental lifetimes of excited states, reduced transitional probability $B(E2)$, and transitional quadrupole moments Q_t for the positive- and negative-parity bands of ^{75}Kr obtained in the present experiment. Excitation energies (E_x), γ-ray energies (E_γ), and spins were taken from Ref. [12].

E_x (keV)	I_f^π ($\hbar$)	I_i^π ($\hbar$)	E_γ (keV)	Previous work (ps)	τ_{148} (ps)	τ_{32} (ps)	$\tau_{\rm acc}$ (ps)	$B(E2)$ (W.u.)[a]	Q_t (e b)
1594	$15/2^+$	$11/2^+$	824	<0.5	$0.687^{+0.035}_{-0.037}$	$0.726^{+0.035}_{-0.036}$	$0.706^{+0.035}_{-0.037}$	163^{+9}_{-8}	$3.53^{+0.10}_{-0.08}$
1963	$17/2^+$	$13/2^+$	896	<0.9	$0.424^{+0.012}_{-0.034}$	$0.418^{+0.017}_{-0.039}$	$0.421^{+0.017}_{-0.039}$	179^{+18}_{-7}	$3.54^{+0.18}_{-0.07}$
2629	$19/2^+$	$15/2^+$	1035		$0.199^{+0.016}_{-0.020}$	$0.177^{+0.023}_{-0.023}$	$0.188^{+0.023}_{-0.023}$	195^{+27}_{-21}	$3.59^{+0.24}_{-0.20}$
3049	$21/2^+$	$17/2^+$	1086		$0.185^{+0.005}_{-0.019}$	$0.152^{+0.006}_{-0.007}$	$0.168^{+0.005}_{-0.019}$	172^{+22}_{-5}	$3.30^{+0.20}_{-0.05}$
3824	$23/2^+$	$19/2^+$	1195		$0.136^{+0.013}_{-0.018}$	$0.192^{+0.031}_{-0.025}$	$0.164^{+0.031}_{-0.025}$	169^{+31}_{-27}	$3.22^{+0.28}_{-0.27}$
4277	$25/2^+$	$21/2^+$	1128		$0.137^{+0.005}_{-0.006}$	$0.093^{+0.010}_{-0.010}$	$0.115^{+0.010}_{-0.010}$	136^{+13}_{-11}	$2.85^{+0.13}_{-0.12}$
5025	$27/2^+$	$23/2^+$	1201		<0.167	<0.122	<0.144	>121	>2.67
5558	$29/2^+$	$25/2^+$	1281		$0.129^{+0.009}_{-0.010}$	$0.062^{+0.013}_{-0.018}$	$0.096^{+0.013}_{-0.018}$	132^{+30}_{-16}	$2.76^{+0.11}_{-0.10}$
6891	$33/2^+$	$29/2^+$	1333		<0.099	<0.109	<0.104	>100	>2.37
1646	$13/2^-$	$9/2^-$	741	1.0(3)	$1.252^{+0.073}_{-0.069}$		$1.252^{+0.073}_{-0.069}$	156^{+9}_{-9}	$3.25^{+0.09}_{-0.09}$
2109	$15/2^-$	$11/2^-$	844	<0.6	$0.627^{+0.061}_{-0.050}$		$0.627^{+0.061}_{-0.050}$	163^{+14}_{-15}	$3.22^{+0.13}_{-0.15}$
2562	$17/2^-$	$13/2^-$	916		$0.415^{+0.043}_{-0.039}$	$0.359^{+0.037}_{-0.039}$	$0.387^{+0.043}_{-0.039}$	175^{+22}_{-17}	$3.27^{+0.20}_{-0.17}$
3110	$19/2^-$	$15/2^-$	1001		$0.236^{+0.025}_{-0.035}$	$0.253^{+0.020}_{-0.020}$	$0.245^{+0.025}_{-0.035}$	177^{+20}_{-16}	$3.24^{+0.18}_{-0.15}$
3623	$21/2^-$	$17/2^-$	1061		<0.213	<0.200	<0.207	>157	>3.02
4290	$23/2^-$	$19/2^-$	1180		$0.138^{+0.012}_{-0.019}$	$0.178^{+0.038}_{-0.046}$	$0.158^{+0.038}_{-0.046}$	120^{+38}_{-23}	$2.63^{+0.39}_{-0.27}$
5464	$27/2^-$	$23/2^-$	1174		<0.197	<0.230	<0.213	>92	>2.26

[a]W.u. = 18.79 e^2 fm^4.

in the target and in the backing with a time step of 0.01 ps for 10,000 histories of energy losses at different depths. Shell-corrected Northcliffe and Schilling [18] electronic stopping powers have been used for calculating the energy loss. In the analysis of both of the bands, an effective lifetime was obtained for the topmost level by assuming a prompt feed to this level; for the rest of the transitions we have used a rotational cascade side-feeding model of five transitions with a fixed moment of inertia of $20\hbar^2$ MeV^{-1} throughout the analysis. The intensities of side-feeding transitions and branching ratio for the positive- and negative-parity bands were obtained from experimentally determined relative intensities listed in Ref. [12]. The transition quadrupole moments for the side-feeding bands Q_t(SF) were found to be $\sim$2.4(6) e b for the positive-parity bands and $\sim$2.0(5) e b for the negative-parity bands from fits to the experimental line shapes. Lifetimes were determined by analyzing the Doppler-broadened line shapes of the transitions (see Table I) in 148° and 32° coincidence spectra. The line shapes of most of the transitions in the favored signature of the positive-parity band have been obtained with a gate on the 191-keV transition, de-exciting the $9/2^+$ state of this band. However, for the 1228- and 1281-keV transitions the gate on the 896-keV transition has been used to minimize the interference of the 1201- and 1284-keV transitions present in the unfavored signature band. The line shapes of lower transitions of the unfavored signature band were obtained with a gate on the 392-keV ($11/2^+ \rightarrow 9/2^+$) transition. The line shapes of the 1195- and 1201-keV transitions were obtained using a sum gate on $\Delta I = 1$ transitions with energies of 527 and 665 keV in this band and fitting them together. In negative-parity bands, the lifetimes of $13/2^-$ and $15/2^-$ states have been obtained from coincidence spectra gated on transitions above the level of interest in the 90° detectors. This procedure is used to remove the effect of other interband transitions with energies of 741, 844, and 848 keV (feeding the $5/2^-$, $11/2^-$, and $11/2^-$ states, respectively, of this negative-parity band) on the line shapes of the 741- and 844-keV transitions, which are emitted from $13/2^-$ and $15/2^-$ states, respectively. Lifetimes of other states above the $15/2^-$ were determined by gating below the transition of interest. The experimental and fitted line shapes for some representative transitions at 148° and 32° are shown in Fig. 1.

The measured lifetimes of levels in the positive- and negative-parity bands were obtained by taking the arithmetic averages of the results measured at 148° and 32° and are listed in Table I. Reduced electric quadrupole transition probability $B(E2)$ values obtained from the measured lifetimes and the resulting transition quadrupole moment Q_t values are listed in the last two columns of Table I, respectively. The values of spin projection quantum numbers $K = 5/2$ and $K = 3/2$ were used for the positive- and negative-parity bands, respectively. The plot of moment of inertia as a function of rotational frequency indicates some irregularities around $\hbar\omega = 0.63$ MeV ($I = \frac{25}{2}\hbar$) for the positive-parity band and around $\hbar\omega = 0.57$ MeV ($I = \frac{23}{2}\hbar$) for the negative-parity band, which was noticed in the cranking model and interpreted as $g_{9/2}$ proton alignment in the previous work [12].

Figures 2 and 3 show the variation of transition quadrupole moments for positive- and negative-parity bands as a function

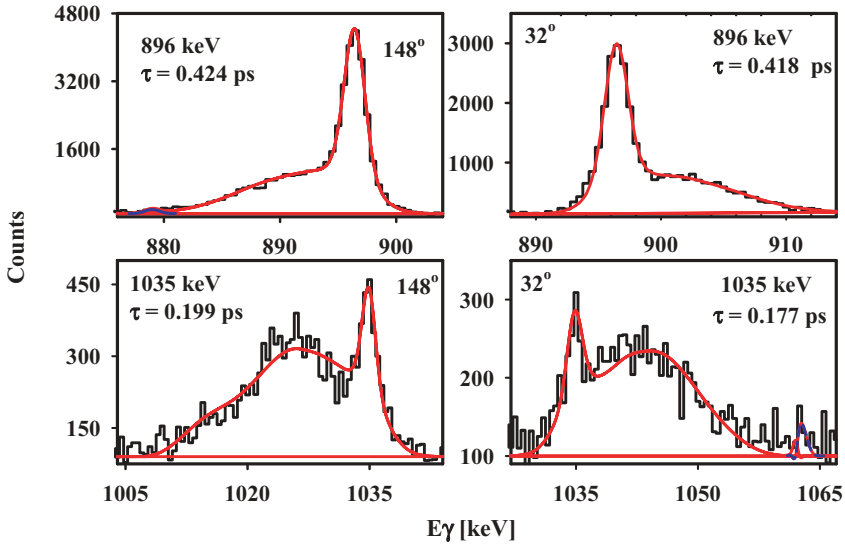

FIG. 1. (Color online) Least-squares fits of line shapes of some representative transitions (896 and 1035 keV) of ^{75}Kr. The left-hand frames show the data for the 148° detectors and right-hand frames show the data for 32° detectors. The contaminant peaks are shown by dotted lines.

of spin. The behaviors of both signature partners are almost same in both parity bands. The average values of transitional quadrupole moments are 3.5 and 3.2 e b for positive- and negative-parity bands, respectively, before the band crossing. The present work also reports the Q_t measurements for few states beyond the band-crossing region. Though these limited data points indicate some systematic reduction in Q_t values beyond the band crossing, further measurements are required to produce a concrete picture of the evolution of collectivity with particle alignment.

The PSM [13], used for understanding the evolution of collectivity of ^{75}Kr up to high spins, is based on the Hamiltonian given by

$$\hat{H} = \hat{H}_0 - \frac{1}{2}\chi \sum_{\mu} \hat{Q}^{\dagger}_{\mu}\hat{Q}_{\mu} - G_M \hat{P}^{\dagger}\hat{P} - G_Q \sum_{\mu} \hat{P}^{\dagger}_{\mu}\hat{P}_{\mu}. \quad (1)$$

Here, $\hat{H}_0$ is the spherical single-particle Hamiltonian, which contains a proper spin-orbit force. The monopole pairing strength G_M is taken to be $G_M = [G_1 - G_2(N-Z)/A]/A$ for neutrons and $G_M = G_1/A$ for protons with $G_1 = 18.23$ and $G_2 = 15.12$. To compare these pairing strengths to those used in the previous PSM calculations for even-even nuclei in the same mass region (see, e.g., Refs. [19,20]), the pairing strengths employed in this work are reduced by a factor of 0.90 for G_1 and 0.94 for G_2 to take into account the weakened pairing in odd-mass systems attributable to the blocking effect. The quadrupole pairing strength G_Q is assumed to be 0.16 times G_M. Finally, the quadrupole-quadrupole interaction strength χ is determined by the self-consistent relation associated with deformation ε_2 [13]. The value of deformation $\varepsilon_2 = 0.365$ is used to construct the deformed Nilsson basis.

As the valence space for this mass region, particles in three major shells ($N = 2, 3, 4$ for both neutrons and protons) are considered. For the low-lying bands of odd-even nuclei, the quasiparticle (qp) configuration space $|\phi_\kappa\rangle$ consists of a set of 1-qp and 3-qp states,

$$|\phi_\kappa\rangle = (\alpha^{\dagger}_{n_i}|0\rangle,\ \alpha^{\dagger}_{n_i}\alpha^{\dagger}_{p_j}\alpha^{\dagger}_{p_k}|0\rangle), \quad (2)$$

where $\alpha^{\dagger}$ is the creation operator for a qp and the index n (p) denotes neutron (proton) Nilsson quantum numbers that run over the orbitals close to the Fermi levels.

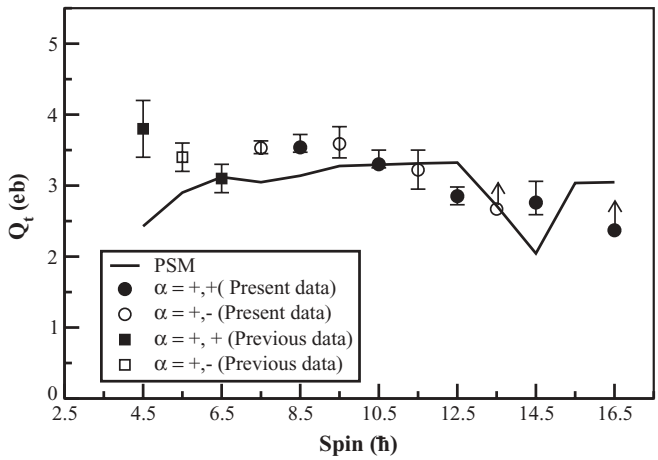

FIG. 2. Comparison of the measured transitional quadrupole moments Q_t for excited states in the positive-parity bands in ^{75}Kr with the prediction of the projected shell-model calculation.

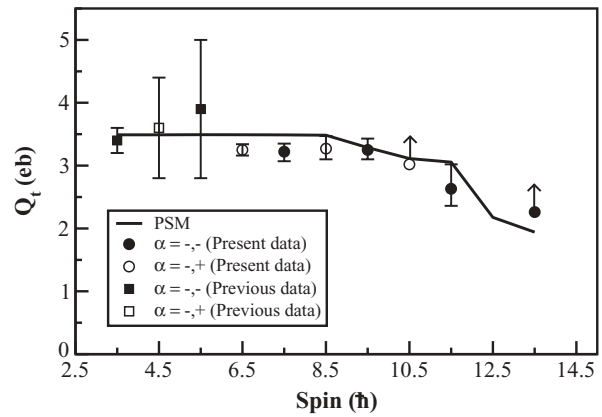

FIG. 3. Comparison of the measured transitional quadrupole moments Q_t for excited states in the negative-parity bands in ^{75}Kr with the prediction of the projected shell-model calculation.

The variation of transitional quadrupole moments with spin for the positive- and negative-parity bands are compared to the calculations, in Figs. 2 and 3, respectively. For completeness, the present measurements of transitional quadrupole moments (see Table I) for spin above $I^\pi = 15/2^+$ for the positive-parity band and $I^\pi = 13/2^-$ for the negative-parity band are plotted along with the previous measurements from Ref. [12]. It is found that the moments Q_t for both positive- and negative-parity bands have rather similar values at low spins. At high spins, in particular after the 1-qp and 3-qp band crossing, Q_t clearly decreases. The decrease in transition quadrupole moment corresponds to a quenching of system deformation.

For the lowest spin states of positive parity the calculated values underpredict the previous measured Q_t values, as seen in Fig. 2. This discrepancy in Q_t can be attributed to our simplified description of the deformed basis. A similar problem was found for the even-even nuclei of the same mass region [20]. In the present PSM calculation for ^{75}Kr, a fixed prolate deformation is assumed. It is known that this nucleus is characterized by shape changes at low spins [12]. This means that, near the ground state, the potential energy surface has a soft character, which cannot be ideally modeled by a single deformation. For the negative-parity band the transitional quadrupole moments (Q_t) remain constant up to the band-crossing region and then decrease slightly by $\approx$13%. This trend is quite nicely reproduced by the calculated (Q_t) values of PSM, as shown in Fig. 3.

For the positive-parity states, we find that the neutron 1-qp band of $\frac{5}{2}$[402] lies lowest in energy in the low-spin region, whereas the other two, the 1-qp $\frac{1}{2}$[420] and $\frac{3}{2}$[402] bands, lie, respectively, about 0.7 and 1.9 MeV above. Thus, the main component in the positive-parity band under discussion should be of $K = \frac{5}{2}$. However, the band cannot retain its pure configuration when the nucleus rotates faster because the 3-qp configurations are seen to be lower, approaching or even crossing the $K = \frac{5}{2}$ band at higher spins. The three important 3-qp bands that are found to be the lowest among many other 3-qp bands are listed in Table II. Around the region of band crossing, the corresponding wave functions must undergo a configuration change because of band mixing. The changes in configuration can lead to reduced Q_t values near that spin (as seen in Fig. 2). Similar variations discussed earlier in this report happen also in the negative-parity band. The lowest band is the neutron 1-qp $\frac{3}{2}$[321] band. The other two 1-qp bands, the $\frac{3}{2}$[312] and $\frac{5}{2}$[312] bands, lie about 1.5 MeV above it. At $I = 25/2$, the calculation predicts a crossing of the $\frac{3}{2}$[321] band by two 3-qp bands (see the configurations listed in Table II). Because of this crossing, a similar reduction in Q_t is expected, as in the positive-parity case. A detailed PSM analysis of the nearby odd-A nuclei will be presented in a forthcoming article to get a systematic picture of shape evolution in this region [21].

TABLE II. Important configurations of 1- and 3-qp states used in band mixing of positive- and negative-parity bands.

Parity	qp	Total K	Configurations
+	1-qp	5/2	ν 5/2[402]
		1/2	ν 1/2[420]
		3/2	ν 3/2[402]
+	3-qp	3/2	ν 5/2[402] $\oplus$ π 1/2[400] $\oplus$ π 3/2[402]
		7/2	ν 5/2[402] $\oplus$ π 1/2[400] $\oplus$ π 3/2[402]
		5/2	ν 3/2[402] $\oplus$ π 1/2[400] $\oplus$ π 3/2[402]
−	1-qp	3/2	ν 3/2[321]
		5/2	ν 5/2[312]
		3/2	ν 3/2[312]
−	3-qp	1/2	ν 3/2[321] $\oplus$ π 1/2[400] $\oplus$ π 3/2[402]
		5/2	ν 3/2[321] $\oplus$ π 1/2[400] $\oplus$ π 3/2[402]

In summary, lifetimes of the high-spin states have been measured via the ^{50}Cr(^{28}Si,2pn)^{75}Kr reaction, for the yrast positive- and negative-parity bands of ^{75}Kr. The extracted transitional quadrupole moments for both bands remain constant before the band crossing. The experimental values of transition quadrupole moments have been compared with the predictions of PSM and provide a good description of the measured data. Further measurements of the lifetime of excited states up to higher spins for this nucleus are required to quantify the effect of particle alignment on the evolution of collectivity.

We thank the staff members of the Pelletron facility and target laboratory of IUAC. Financial support by IUAC (UFUP-41311) is gratefully acknowledged. Research at SJTU (Y.-C.Y. and Y.S.) was supported by the National Natural Science Foundation of China under Contract No. 10875077.

[1] C. J. Lister, B. J. Varley, H. G. Price, and J. W. Olness, Phys. Rev. Lett. **49**, 308 (1982).
[2] S. M. Fischer *et al.*, Phys. Rev. Lett. **84**, 4064 (2000).
[3] R. Palit, H. C. Jain, P. K. Joshi, J. A. Sheikh, and Y. Sun, Phys. Rev. C **63**, 024313 (2001).
[4] W. Nazarewicz *et al.*, Nucl. Phys. **A435**, 397 (1985).
[5] T. D. Johnson *et al.*, Phys. Rev. C **42**, 2418 (1990).
[6] A. Dhal *et al.*, Eur. Phys. J. A **27**, 33 (2006).
[7] R. A. Kaye *et al.*, Phys. Rev. C **69**, 064314 (2004).
[8] R. A. Kaye *et al.*, Phys. Rev. C **66**, 054305 (2002).
[9] G. Mukherjee *et al.*, Z. Phys. A **359**, 111 (1997).
[10] C. J. Gross *et al.*, Phys. Rev. C **49**, R580 (1994).
[11] M. A. Cardona, G. Garcia Bermudez, A. Filevich, and E. Achterberg, Phys. Rev. C **42**, 591 (1990).
[12] S. Skoda *et al.*, Nucl. Phys. **A633**, 565 (1998).
[13] K. Hara and Y. Sun, Int. J. Mod. Phys. E **4**, 637 (1995).
[14] Y. Sun and H. Hara, Comput. Phys. Commun. **104**, 245 (1997).
[15] G. K. Mehta *et al.*, Nucl. Instrum. Methods A **268**, 334 (1988).
[16] S. Muralithar *et al.* (submitted for publication).
[17] J. C. Wells, ORNL Physics Division Progress, Report No. ORNL-6689, September 30, 1991.
[18] L. C. Northcliffe and R. F. Schilling, At. Data Nucl. Data Tables **7**, 233 (1970).
[19] R. Palit *et al.*, Nucl. Phys. **A686**, 141 (2001).
[20] Y. Sun, Eur. Phys. J. A **20**, 133 (2004).
[21] Y. Sun *et al.* (in preparation).